Journal of the European Ceramic Society xxx (xxxx) xxx–xxx

Contents lists available at ScienceDirect

Journal of the European Ceramic Society

journal homepage: www.elsevier.com/locate/jeurceramsoc

Thermal and mechanical cyclic tests and fracture mechanics parameters as indicators of thermal shock resistance – case study on silica refractories

K. Andreev[a,*], V. Tadaion[a,b], Q. Zhu[c], W. Wang[c], Y. Yin[c], T. Tonnesen[b]

[a] Ceramics Research Centre, Tata Steel Europe, 1951MD, Velsen Noord, The Netherlands
[b] Institute of Mineral Engineering, RWTH Aachen University, 52070, Aachen, Germany
[c] The State Key Laboratory of Refractories and Metallurgy, Wuhan University of Science and Technology, 430081, Wuhan, China

ARTICLE INFO

Keywords:
Fused silica refractories
Brittleness
Thermal shock resistance
Fracture energy
Strain controlled fatigue

ABSTRACT

The paper discusses alternative methods to assess thermal shock in refractories. Thermal shock performance of two conventional silica bricks and two novice fused silica materials has been studied. Methods involving fracture mechanical tests of monotonic loading, repetitive thermal shock tests and cyclic strain controlled fatigue tests have been utilised. The amorphous fused silica is rather brittle. However low thermal expansion guarantees its superior thermal shock resistance. In-service crystallisation is to happen rather quickly. For crystallised fused silica of the studied morphology the tests coherently predict superior thermal shock resistance due to less brittle failure. Strain controlled fatigue test allows assessment of strain limits in the conditions of cyclic loading and thus combines the benefits of the thermal shock and monotonic fracture mechanics tests. Strain tolerance seems to be the property to correlate the results of the alternative test methods and those with the service loads.

1. Introduction

During the service in insulating linings of high temperature industrial units refractories are often exposed to periodic thermal-shock. It is the state of the art to evaluate the resistance of refractories to temperature fluctuations by fracture mechanics based indexes of merit [1–4]. The indexes combine the physical properties and fracture mechanical parameters obtained in monotonic stress-strain tests. Alternatively, the thermal shock test when a sample is exposed to periodic temperature fluctuations is used to study the effect of repetitive thermal shock events [5–9]. The damage is quantified by the loss of strength and by non-destructive tests. For refractories such tests seldom feature more than several dozen cycles [5,9]. Mechanical cyclic tests can simulate several thousand cycles. They are used to study fatigue degradation [6,10–16]. The degradation is typically judged from the stress-strain parameters, such as irreversible strains. Cyclic stress-strain measurements performed at discrete temperatures are largely representative for the failure due to temperature fluctuations [17,18]. For the above three approaches similar ranking order was obtained for selected materials when their parameters of linear elastic fracture mechanics (LEFM), data on stress-controlled fatigue in uni-axial compression and thermal shock experiments were compared [6,10]. No studies on the correlation of strain controlled fatigue measurements and other methods are known to the authors.

Conventional silica bricks are known for their dimensional stability at high temperature and resistance to acidic slag [19,20]. The bricks are produced from quartzite by pressing and high temperature sintering. The main drawback of these materials is high thermal expansion at low temperatures and resulting sensitivity to fluctuations in wider temperature range [7,21,22]. To overcome the deficiency of the conventional bricks fused silica based materials have been developed [19]. They may feature different binders, including cement, silica gel and phosphates, and can be produced either by pressing or casting. The main features of fused silica refractories are low coefficient of thermal expansion and the possibility to obtain large and complex pre-cast shapes. Their drawback is the potential crystallisation of silica at high temperature and the limited service statistics. The latter necessitates thorough research of the material properties. Properties of silica bricks has been extensively studied over years [7,16,20,23–25]. Limited amount of data available for fused silica is mainly for the material in its original amorphous condition [21,26,27]. Three point bending tests done at room temperature performed on samples of silica brick and crystallised fused silica material has indicated a rather brittle failure for the former and developed strain softening for the latter [27]. The fatigue in silica brick is affected by grain interlocking [13], large grain cracking [13] and the damage healing by the melt formation [16].

The paper discusses alternative methods to study thermal shock using the example of silica refractories. Thermal shock resistance of two

* Corresponding author.
E-mail address: Kirill.Andreev@tatasteel.com (K. Andreev).

https://doi.org/10.1016/j.jeurceramsoc.2018.12.062
Received 29 October 2018; Received in revised form 24 December 2018; Accepted 29 December 2018

novice fused silica materials and two conventional silica bricks was measured. Fused silica materials were tested in as delivered amorphous form and after crystallisation achieved by additional heat treatment. Measurements according to the alternative methods were conducted at three cooperating labs according to the established procedures. Fracture mechanics parameters were obtained from the wedge splitting test according to Tschegg [28,29]. The degradation due to cyclic loading was assessed by the thermal shock experiments and strain controlled fatigue measurements. The latter were done in three point bending set-up. The analysis was supported by basic physical and chemical tests, the measurements of thermal expansion and dynamic Young's modulus. XRD was used to quantify the mineralogical composition of the original materials and fused silica after high temperature crystallisation. The discussion on the alternative methods to study thermal shock is seen as beneficial for establishing a link between the service loads and material properties. The latter is especially important for selecting the materials for linings of lengthy campaign life, as for those where silica refractories are used.

2. Materials

2.1. Materials

Four commercially available silica refractories are investigated. All the materials are used in coke ovens of steel industry. Similar refractories are also used in hot blast stoves serving blast furnaces and glass producing units [19]. The maximal service temperature is typically between 1100 and 1400 °C. Two of the studied materials (SB1, SB2) are conventional silica bricks produced by pressing with calcium hydroxide acting as a binder. Their sintering is done at 1400–1500 °C. The material SB1 is heat treated at higher temperatures than SB2. It meets stricter specification for residual quartz, which is undesirable in the refractories due to mineralogical transition causing growth [30]. The other two products (FS1, FS2) are based on fused silica. The material FS1 is produced by casting and features calcium-aluminate cement binder. The cast block is dried and heat treated to temperatures below 1200 °C. The material FS2 is produced by pressing. The binder is mono-aluminium phosphate. The bricks are heat treated below 1000 °C. The chemical-physical properties of studied materials are demonstrated in the Results section of the paper.

Samples of fused silica materials were studied in as delivered predominantly amorphous form and after the heat treatment at 1400 °C for 100 h. The heat treatment was to achieve crystallisation expected to occur during the service. To prevent cracking of the heat treated fused silica samples the average cooling rate after the heat treatment was approximately 10 °C/h. Further in the paper the "crystallised" fused silica means the material heat treated in the regime 1400 °C/100 h. The abbreviations for crystallised fused silica materials are CFS1 and CFS2.

2.2. Methods and equipment

The chemical and mineralogical composition was determined by XRF and XRD (Rietveld) methods using powders. The progress of crystallisation was measured on fused silica samples after the conditioning at 1400 °C for 24, 48 and 100 h. The XRD patterns were recorded in the range of 10 to 130° (2 Θ) in reflection mode using a fully automated Bruker D4 diffractometer (CoK_{α}-radiation) equipped with a position sensitive detector. The step size was n.d.0.02°, time per step was 200 s. Quantitative determination of phase proportions was also performed by Rietveld analysis. The refinement was done on the assumption of pure phases. Unit cell parameters, background coefficients, preferred orientations, profile parameters and phase proportions were refined using the TOPAS software package for Rietveld refinement. Apparent density and open porosity was measured by the water immersion method according to EN993-1. Thermal expansion was measured according to ISO 1893. Samples were cylinders with a diameter of 50 mm and the height of 50 mm. The diameter of the axial channel was 13 mm. The heat-up rate was 4 °C/min. The constraining pressure was 0,02 MPa. The dynamic Young's modulus was obtained by the impact excitation technique in the Resonant Frequency Damping Analyser (RFDA) by IMCE BV. The typical sample geometry was 25 × 25 × 120 mm3. The measurements were done between room temperature (RT) and 1300 °C during cooling and heating with the rate of 4 °C/min. The technique and formulas to calculate the Young's modulus from the out-of-plane flexure mode resonant frequency are described in [31]. The thermal conductivity and heat capacity was measured by cross wire method according to EN993-14. The micrographs of the materials were obtained by an automated petrographical microscope Zeiss Axial Imager Z1. Stereo microscope Zeiss Stemi 2000-CS Stereo was used to study cracks after the thermal shock tests. In all cases of heat treatment and high temperature tests the furnace condition accuracy was +/- 0,5% of the current temperature.

The wedge splitting tests according to Tschegg [28,29] were done in a high temperature test frame by Shen Zhen Wance Testing Machine Co. Tests were performed at RT, 800 and 1100 °C. Samples of SB2, FS2 and CFS2 were analysed. The test procedure and the data analysis was as in [32]. Two contact extensometers were used to obtain horizontal displacements. The horizontal force was calculated from the vertical force [32]. The width, depth and height of the samples were 100 mm, 65 mm and 100 mm, respectively. Due to notches the failed cross-section had the width and height of 55 mm and 66 mm, respectively. The tests were performed with vertical wedge displacement rate of 0,5 mm/min. For tests at high temperature the average heat-up rate was 4 °C/min. The holding time was 1 h. It should be stressed that the fracture energy was determined using horizontal displacements measured by the extensometers. If the horizontal displacements calculated from the vertical displacements of the wedge is used for the purpose the obtained fracture energy is somewhat higher. However the shift is consistent and the ranking of the materials is not changed.

Thermal shock experiments were done on the samples of SB1 and CFS1. The prismatic samples of 25 × 25 × 145 mm^3 were used. The tests involved repetitive cooling and heating thermal shock cycles realised by moving the samples between chambers conditioned at 300 and 1200 °C. The in-house developed equipment was used [8]. The conditioning at the temperature subsequent to the shock event was 1 and 2 h in the hot and cold chambers, respectively. Apart from the shock events the cooling and heating rates were 2 °C/min. The degradation was judged by the presence of cracks and from the changes of the dynamic Young's modulus and the residual bending strength (MOR) after 50 cycles. For those measurements the shocked samples were cooled down and conditioned at RT for at least 24 h. In comparison with tests where the thermal cycles are done between one high temperature and the ambient air the tests between the two high temperatures allow more realistic representation of the service conditions.

Monotonic and cyclic three point bending tests were performed in a mechanical test frame by Zwick-Roel equipped with a furnace. Tests were performed at RT and 1000 °C. The loading rate was 0,3 mm/min. The sample geometry was 25 × 25 × 145 mm^3 and the span was 120 mm. In the cyclic tests of constant displacement (strain) amplitude the loading protocol was as in the Method III of [13]. During the loading phase of the cycle the amplitude stays constant. The unloading stops upon reaching the minimal force level. The next loading starts where the previous unloading stopped. The tests were performed with amplitudes ranging between 40 and 100% of the average displacement at failure (displacement at the maximal force) registered in monotonic loading. For samples coming from different bricks the displacement at failure specific for this brick was used. The fatigue tests were done on samples of SB1, SB2, CFS1 and CFS2. Regarding the crystallisation rates discussed in [21] the additional crystallisation of FS1 and FS2 during the conditioning before the high temperature mechanical tests is not expected to exceed 0%, 5% and 15% for tests at 800 °C, 1000 °C and 1100 °C, respectively.

Table 1
Material properties.

	SB1	SB2	FS1	FS2
Chemical composition (main components), %				
SiO_2	96	96	97	98
Al_2O_3	1,0	1,0	< 3	0,5
Fe_2O_3	0,5	0,5	0	0
CaO	2,5	2,5	< 3	0
P_2O_5	0	0	0	0,4
Bulk density, g/cm^3	1,86	1,84	1,83	1,9
True density, g/cm^3	2,34	2,35	2,31	2,29
Apparent porosity, %	19,4	19,6	18,6	14
Thermal expansion, %				
RT-1000 °C	1,2	1,3	0,3/1,3*	0,1/1,4*
Dynamic Young's modulus, GPa				
RT	11	12	6/4*	20/2*
1000 °C	24	28	27/20*	37/11*
Heat conductivity, W/m/K				
RT	1,5	–	1,1/1,3*	–
1000 °C	2,2	–	2,0	–
Heat capacity, W/m/K				
RT	780	–	782	–
1000 °C	1295	–	1207	–

* after the heat treatment 1400 °C/100 h.

3. Results and discussion

3.1. Physical properties

An overview of physical properties and microstructure is given in Tables 1 and 2 and Figs. 1–4. The silica bricks SB1 and SB2 have identical chemical composition. The main mineralogical components are cristobalite, tridymite and potentially quartz. High temperature exposure is known to reduce the quartz content [30] and to promote the transition of cristobalite into tridymite [33]. For SB1 more intensive heat treatment during the production explains higher amount of tridymite and lower amount of quartz than in SB2. High temperature exposure also promotes grain recrystallisation. As a result the microstructure of SB1 does not show any clear difference between large grains and the matrix. In SB2 treated at lower temperature this difference is clear (Fig. 2a, b). For silica bricks reversible transitions of the polymorphs are responsible for the non-linear temperature function of thermal expansion [19,30] and dynamic Young's modulus [23,24] (Fig. 3).

In as delivered form FS1 has higher amount of crystalline phases than FS2 (Table 2). During the production this material received more intensive heat treatment. The crystallisation of fused silica starts at temperatures above 900 °C [19,21]. Upon reaching 1400 °C it is rather advanced (Table 2). During the conditioning at 1400 °C the rates of crystallisation gradually diminish. The morphology of materials after 100 h should be largely representative for the in-service crystallised condition. However, it is not expected to be unique. From the exploitation of silica bricks it is known that due to different thermal conditions the post-mortem morphology may vary even within a single brick [33]. In CFS1 and CFS2 heat treated for 100 h amorphous phase is found only in centres of large grains (Fig. 2c,d,f). Micro-cracks are seen on the periphery of the grains. They form during the cooling after the crystallisation due to the thermal expansion mis-match of the grain centres and the matrix. The lower Young's modulus of CFS1 than of FS1 indicates greater number of micro-cracks in the former. As for silica bricks the temperature function of Young's modulus in fused slica is influenced by the transition of polymorphs. However here, opening and closure of larger micro-cracks is, as described for other refractories in [34], to play a significant role. E.g., the step-wise change of the Young's modulus seen in CFS1 at about 200 °C is larger than in SB1 (Fig. 3b). This change is both due to the polymorph transitions and the micro-crack closure caused by it. Rather high Young's modulus of FS2 correlates well with the low porosity of this material (Table 1). Due to low content of crystalline phases in FS2 the changes of its dynamic Young's modulus during heating is rather smooth (Fig. 3b). Thermal expansion of crystallised fused silica is similar to that of silica bricks (Fig. 3a, Table 1). Presence of crystalline phases in FS1 and FS2 explain non zero expansion of these materials.

Table 1 shows the properties needed to obtain the common thermal shock resistance parameters [1,2,4]. In this paper such parameters are not calculated due to extremely non-linear nature of the thermal expansion and Young's modulus. Average of these properties obtained for wider temperature intervals can be misleading. During thermal shock the maximal load in the sample develops after certain time interval [35]. The material properties at the temperature at that time may be different from the average values.

3.2. Monotonic tests - brittleness of materials

Monotonic wedge splitting and bending tests were performed. The former tests delivered fracture energy necessary to quantify the brittleness (Fig. 4, 5). The latter tests provided the reference for the cyclic fatigue tests (Fig. 6). For all the materials the strength in wedge splitting (maximal stress - SIG NT) is lower than in three point bending (MOR). This can be explained by the fact that the wedge splitting test is a notched test. In some cases MOR and SIG NT show different temperature trends (Figs. 5a and 6). E.g. in SB2 with temperature increase MOR stays approximately constant and SIG NT decreases. Exact nature of the differences is not clear. The wedge splitting test guarantees steady crack growth. Three point bending test does not. The dependence of the result on the condition of a single defect is much higher in the bending test. Higher ratio of fracture energy to SIG NT means higher resistance to sudden failure and lower brittleness [3]. The brittleness reduces in the order from FS2 to SB2 to CFS2 (Fig. 5a). The ratios for the former two materials are rather close to each other and at 1100 °C they overlap. The material CFS2 is much less brittle than the other two materials.

The cohesion between the grains and the condition of micro-cracks can explain the differences between the materials and the changes of

Table 2
Mineralogical composition.

	Cristobalite	Tridymite	Quartz	Pseudo-wollastonite	Anorthite-sodian	Amorphous
SB1, %	21-22	76-77	0,3-0,6	2,0	0	0
SB2, %	28-31	63-66	0,6-0,8	3,0-4,8	0	0
FS1, %						
As received	30,0	0	0	0	< 10	60,0
1400 °C/24h	60,5	0	0	0	3,7	35,8
1400 °C/48h	73,4	0	0	0	3,2	23,4
1400 °C/100 h	81,5	0	0	0	2,9	15,6
FS2, %						
As received	11,0	1,0	0	0	0	78,0
1400 °C/48h	67,0	2,5	0	0	0	30,5
1400 °C/100 h	77,0	8,5	0	0	0	14,5

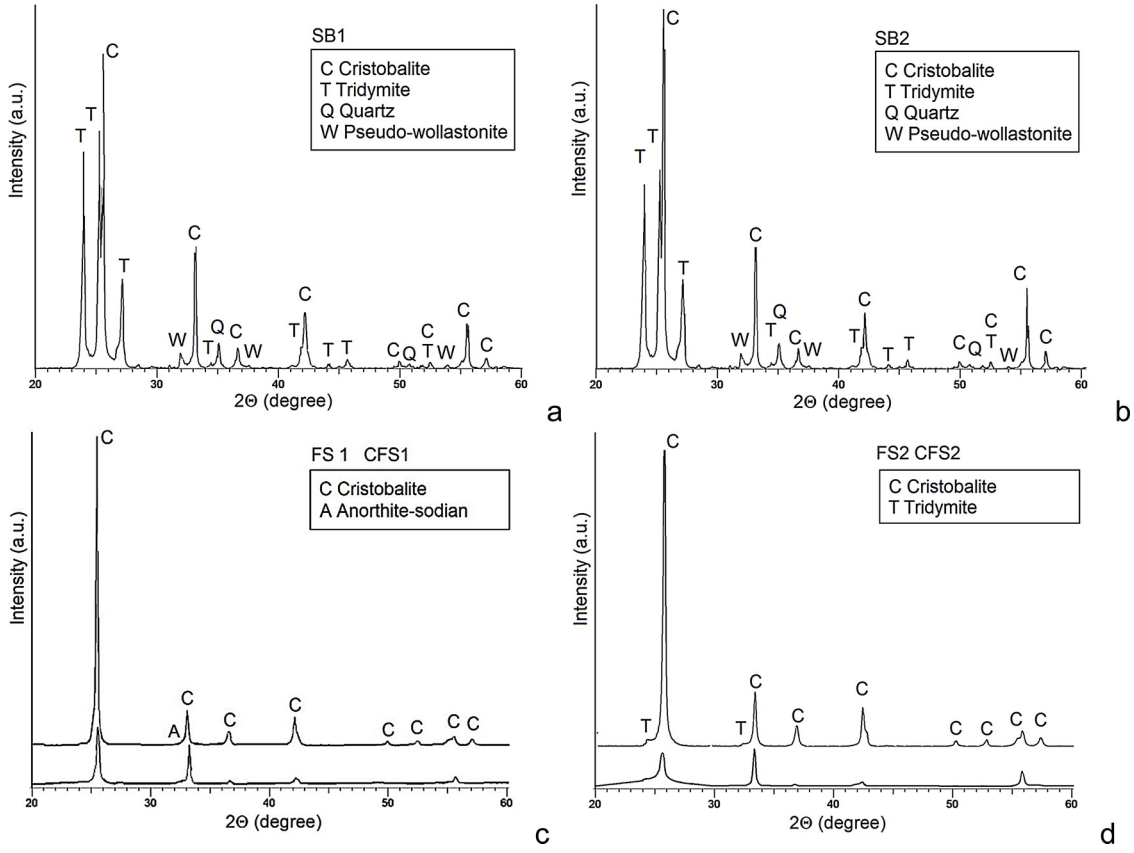

Fig. 1. XRD patterns of (a) SB1, (b) SB2, (c) FS1 and CFS1, (d) FS2 and CFS2.

the material properties with temperature. In refractories the presence of large strong grains and micro-cracks on their periphery and in the matrix of smaller grains resist the instant brittle failure [3,4]. Silica bricks are brittle as the grain cohesion is high and there are few micro-cracks. The latter is due to minimal thermal expansion mis-match between the large grains and the matrix. With increasing temperature, due to proportional reduction of SIG NT and the fracture energy, the brittleness of SB2 stays approximately constant (Fig. 5a).

As it was discussed above the crystallised fused silica has more micro-cracks than the amorphous fused silica. Due to this it has higher fracture energy, lower strength and brittleness (Figs. 5a, 6). With increasing temperature the fracture energy increases and brittleness decreases both in amorphous and crystallised fused silica (Fig. 5a). From growing Young's modulus (Fig. 3a) it can be supposed that the temperature increase causes closure of the micro-cracks. In such condition the micro-cracks still promote the favourable branching of the crack. However, the energy consumed in the crack wake is much higher due to higher friction.

Loads in the refractory lining structures are of the strain controlled nature [3,4]. The quantification of strain tolerance of alternative refractory materials is essential. The comparison of the sample brittleness and the displacement at failure (at maximal force) indicate certain correlation (Fig. 5b). This must be due to the strain hardening resulting from the capacity to sustain growing loads even after the initiation of cracking. The higher is the resistance against an instant crack propagation the higher is strain hardening and higher is the displacement at failure.

3.3. Thermal cyclic tests

According to standards [5] the material is more thermal shock resistant if during thermal cycles it develops no cracks and demonstrates lower loss of Young's modulus and higher residual strength. The material CFS1 is a more thermal shock resistant material than SB1 (Fig. 7, 12). After 50 cycles the average residual MOR for CFS1 and SB1 is 71% and 37%, respectively. The coefficient of variation for MOR is 90% and 10% for SB1 and CFS1, respectively. The high spread of MOR in SB1 is explained by fact that the bending cracks leading to failure coincided with the cracks formed during thermal shock (Fig. 7). The layout of the thermal shock cracks in SB1 is very irregular. Despite the cracks all tested samples kept their integrity and stayed as one piece. Thus the performed tests did not allow determining the amount of cycles to total failure. The samples of CFS1 failed in a more regular manner as there were only few thermal shock cracks. In one sample CFS1-1 (Fig. 7) the bending crack only partially coincides with the thermal sock crack. Thus the position of the pre-crack did not fully define the trajectory of the major crack. The observed cracks in CFS1 were not very deep.

Throughout the cycles the samples of CFS1 showed lower loss of Young's modulus than SB1 (Fig. 12). The degradation of the Young's modulus is presented as damage $D = 1\text{-}E_i/E_0$, where E_0 and E_i are Young's modulii before the test and after the i-th cycle, respectively. In some samples after first two cycles the Young's modulus was higher than in the original condition. The increase is expected to be due to partial healing of the original damage. For those samples E_0 was the Young's modulus after the 2nd cycle. The degradation rates reduce with cycles (Fig. 12). The saturation of damage is typical for tests of repetitive thermal shock [9]. In our case between 30 and 50 cycles the Young's modulus dropped by 1,7 + /-0.9% for SB1 and by 2,6 + /-0,7% for CFS1. Between 15 and 30 cycles the change for FS1 was 4,6 + /-1,7%. For SB1 the drop was around 2,5% for two samples and around 12% for the other two samples. These data demonstrate the slowing down of the damage process. No complete saturation of the damage was observed. The residual Young's modulus correlates well with the residual MOR (Fig. 7). In [36,37] the relationship between the thermal shock damage and residual strength was successfully fit by a power low.

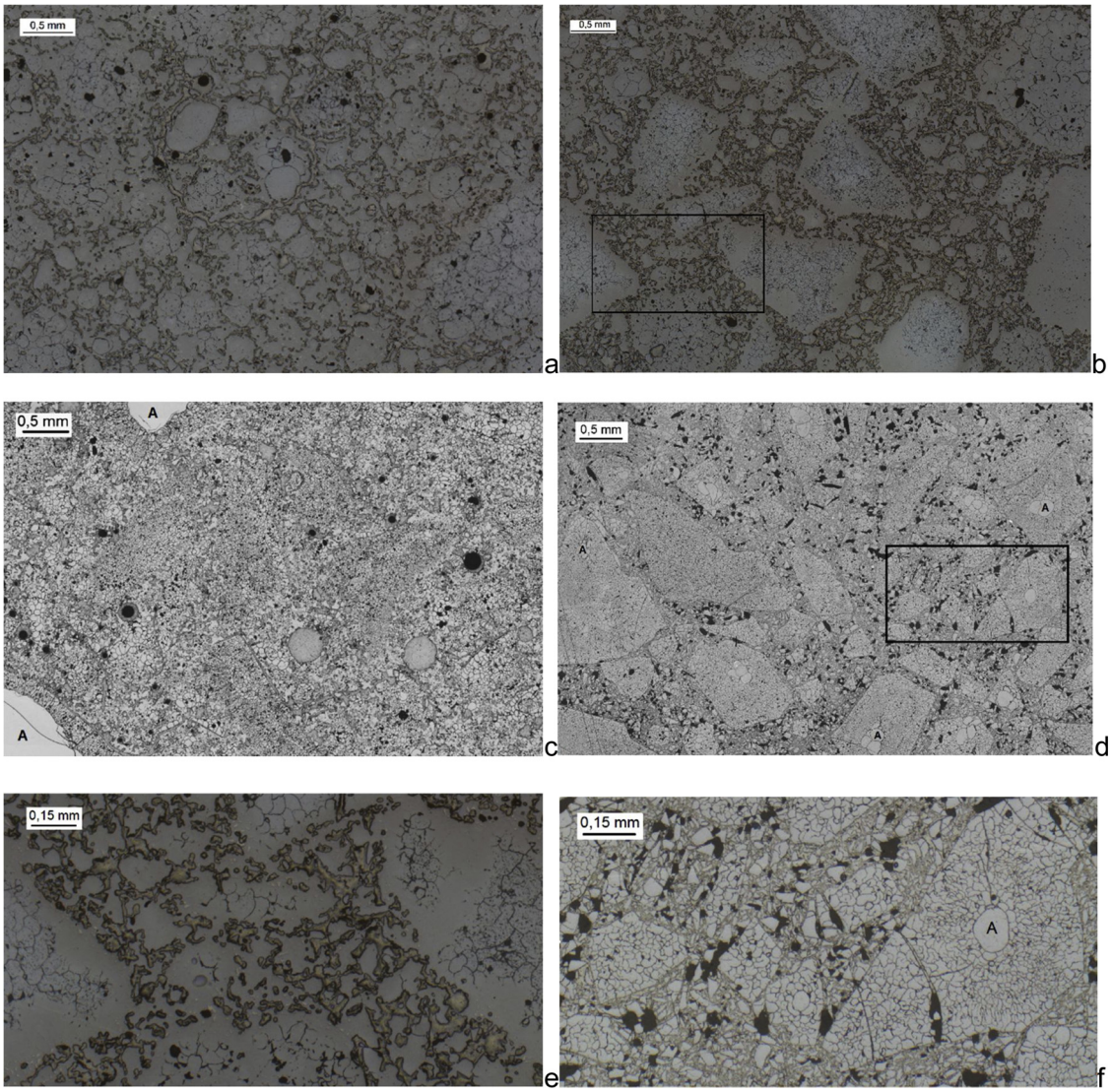

Fig. 2. Typical microstructure of (a) SB1, (b,e) SB2, (c) CFS1, (d,f) CFS2. "A" marks amorphous phase.

In our data the relationship seems to be linear. The sample SB1-4 shows deviation from the trend. Here the MOR crack coincided with the thermal shock crack at the end of the sample (Fig. 7). Such crack has apparently lower effect on the dynamic Young's modulus.

The observation of the samples after thermal shock indicate qualitative differences in the crack trajectories (Fig. 8). In CFS1 cracks have tortuous paths. In such a crack the friction between the sides is rather high which increases the resistance to failure. In SB1 the cracks are rather straight and trans-granular cracks are frequent.

3.4. Mechanical cyclic (fatigue) tests

The fatigue data presents the number of cycles to failure (Figs. 9 and 10) and damage accumulation patterns (Fig. 11) for the wide range of amplitudes. In this way the present set of fatigue data is broader than the sample degradation patterns for one thermal shock regime

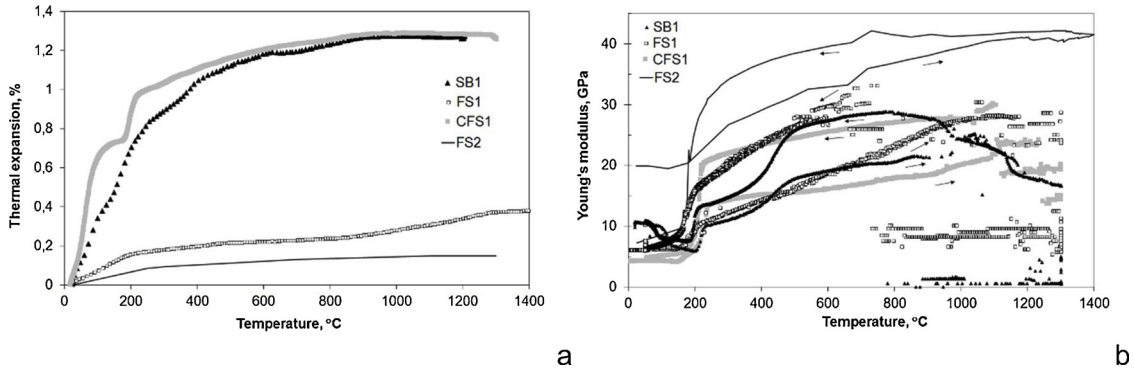

Fig. 3. Thermal expansion (a) and dynamic Young's modulus (b); in (b) the arrows indicate heating and cooling.

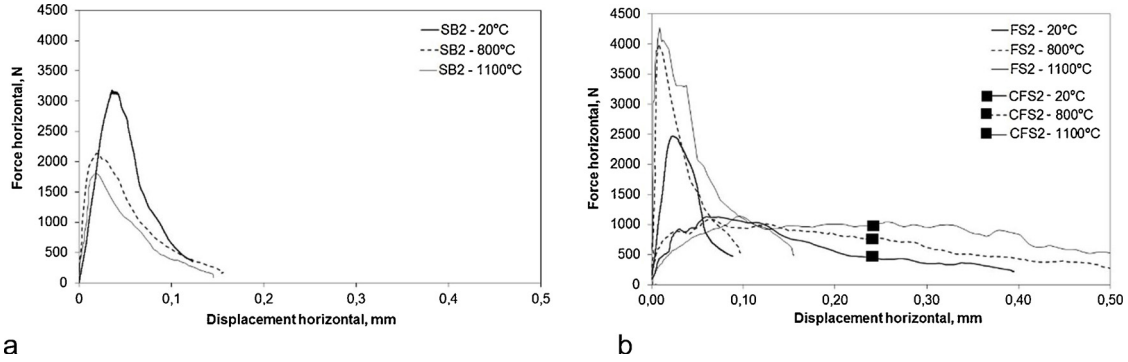

Fig. 4. Typical wedge splitting curves (a) SB2, (b) FS2 and CFS2.

discussed in the section 3.3. Constant strain amplitude of fatigue tests resembles the repetitive strain loads developing during the thermal shock. The more fatigue cycles material can sustain at higher strain amplitude the more robust it is against the thermal shock failure. Thus CFS1 and CFS2 are more thermal shock resistant materials than SB1 and SB2 (Fig. 9, 10). The failure after equal amount of cycles occurs in silica bricks at lower amplitudes than in CFS1 and CFS2. The difference is especially significant for the tests at 1000 °C (Fig. 10b). When the fatigue results for all materials are put in one graph one can see two trends (Fig. 10). One trend is formed by crystallised fused silica materials. The other is formed by silica bricks. The differences seen here must be material type specific.

In cyclic tests the failure occurs at amplitudes as low as 60–70% of the strain at failure in the monotonic loading regime. Lower amplitudes are characterised by higher amount of cycles to failure and steeper correlation trend (Fig. 9, 10). For lowest amplitude tests no failure could be achieved. The spread of the results is increasing with decreasing amplitudes. So for SB1 at RT at the amplitude of 0,16%, 0,14% and 0,13% the failure occurs after 13 + /-5, 195 + /-175 and 1480 + /-1443 cycles, respectively (Fig. 9a). For CFS2 at RT at the amplitudes of 0,25%, 0,22% and 0,19% the failure is after 11 + /-2, 28 + /-23 and 597 + /-786 cycles (Fig. 9d). For the both materials the spread for the lowest amplitude features data for the non-failure samples and is in reality even higher. In [38] higher spread of results at lower amplitudes seen in the samples of refractory concrete was attributed to higher variation in initial damage formed at lower amplitudes.

Formation of damage and its growth under sub-critical loads controls the fatigue degradation [12,27]. The irreversible strains obtained from the stress-strain curves of fatigue tests indicate the damage development (Fig. 11) [13]. In CFS1 and CFS2 the accumulation of the irreversible strains demonstrate three well developed periods. In the first period the rates of strain accumulation decrease. In the second period they are constant. In the third period the irreversible strains increase (Fig. 11b). These are typical phases of fatigue degradation

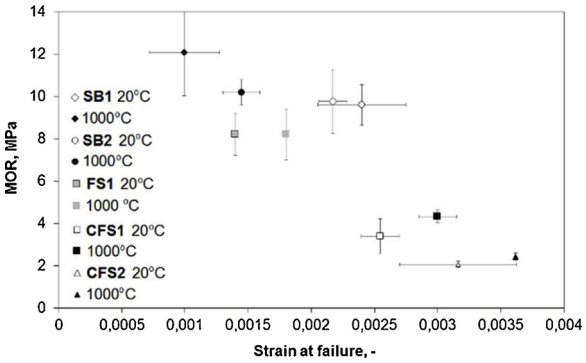

Fig. 6. Results of monotonic three point bending tests.

[12]. On the micro-structural level the primary phase is characterised by the formation and growth of the micro-cracks. The rates of micro-crack growth reduce e.g. due to encountering barriers. During the secondary phase the barriers are overcome by e.g. reducing the friction and the bridging effects in the crack wake [13]. During the ternary phase the cracks may grow together forming the major crack that causes the sample failure. The well-developed third phase should mean extensive resistance to major crack forming and propagation. In SB1 the failure is preceded by multiple cycles that produce very little damage. The primary phase of fatigue is rather short. No ternary phase is present. The failure is sudden, as it is the case with monotonic loading. In SB2 some samples under cyclic regimes show gradual strain softening and the ternary phase of degradation. The development of cyclic strain softening when the material shows sudden failure in monotonic loading was also reported for silica bricks in [13]. To compare the development of damage observed in different methods (Fig. 12) the damage for the mechanical cyclic tests was calculated as $D = EPS_i/EPS_{fin}$, where EPS_i and EPS_{fin} are minimal irreversible strains (end of unloading) for i-th

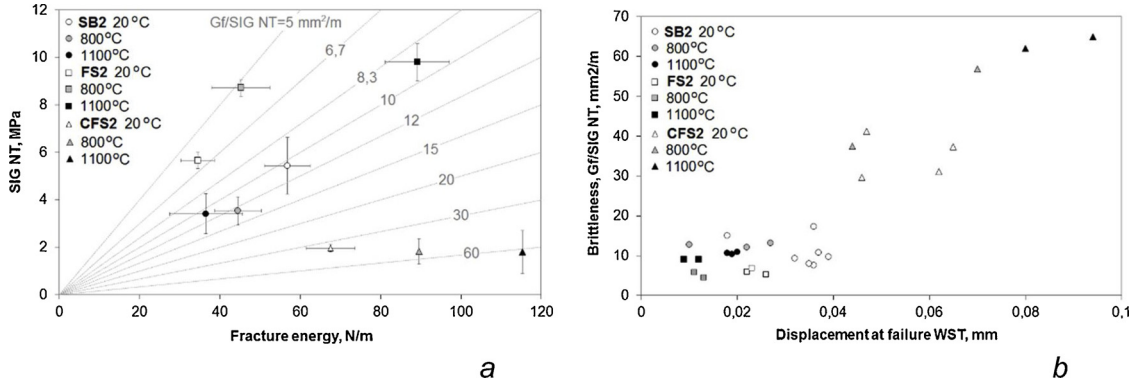

Fig. 5. Results of wedge splitting test.

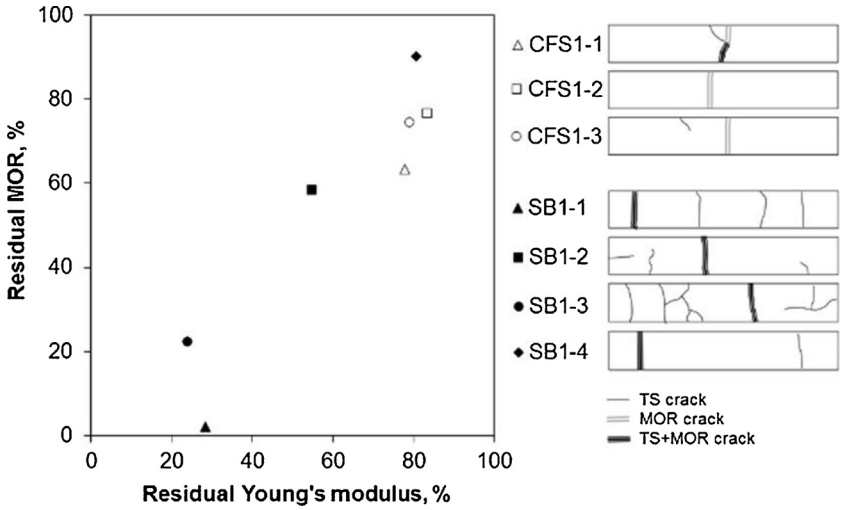

Fig. 7. Correlation of residual dynamic Young's modulus and MOR after 50 thermal cycles, including the schematic representation of cracks in the samples.

cycle and for the last cycle preceding the sample failure. The sample failure is expected when the damage reaches unity.

3.5. Comparison of test methods

Thermal properties (thermal conductivity and heat capacity) and thermal expansion determine the strain loads developing in a material during the temperature fluctuations. Mechanical properties such as brittleness are indicative for the ability to sustain such loads without major crack formation. The fused silica material is to start its service in amorphous condition. Its thermal properties are roughly comparable with those of silica bricks (Table 1). The coefficient of thermal expansion for FS1 and FS2 is some 4–10 times lower than in the bricks (Fig. 3a). The brittleness (Fig. 5), and strain tolerance (Figs. 5, 6), is either similar or at maximum 2 times worse than in the bricks. The difference in thermal expansion is more significant than in other properties. This is to guarantee higher thermal shock resistance of amorphous fused silica. High rates of crystallisation indicate that in service the crystallisation is to occur rather quickly. For this the properties of the crystallised fused silica should be determining for the campaign duration of the refractories. For the crystallised fused silica all utilised methods indicate its superior thermal shock resistance. For this material the effects of the thermal properties and the thermal expansion are accounted for by the thermal shock tests. It should be noted that the material properties of crystallised fused silica after one heat treatment regime was studied here. Further investigation should gain insight into possible crystallised microstructures [39]. The practice to heat treat materials to study the in-service temperature effects is standard for refractories [19]. The practice involves cooling of the material to room temperature and heating it again for the test. In service the material after crystallisation seldom experiences complete cooling. This may result in differences between the in-service crystallised morphology and that of the samples studied by us.

To select the most suitable material and to quantify its performance in given application simple properties based ranking is not always efficient. E.g. even the worst in the list material can be sufficient for some specific application. Refractory linings of short campaign lives provide sufficient in-service performance data to establish a correlation with the material properties. Subsequently this correlation can be used to judge new materials. Silica refractories serve in linings with the expected life of several decennia. For such applications the most efficient approach is to quantify the in-service loads and to compare those with the capacity of the material to bare such loads. To quantify the service loads the strain at critical temperature is seen as a more suitable parameter than temperature or stress. Temperature either outside or inside of the refractory lining is not suitable as thermal shock strains developing in the material depend not only on the temperature and material properties but also on the geometry and intensity of heat exchange [35]. The stresses are less suitable than strains as during the campaign due to the stiffness variation resulting from the damage accumulation the stresses can change significantly. For similar temperature fluctuations the strain amplitudes are to stay constant (or nearly so). Regarding the certain

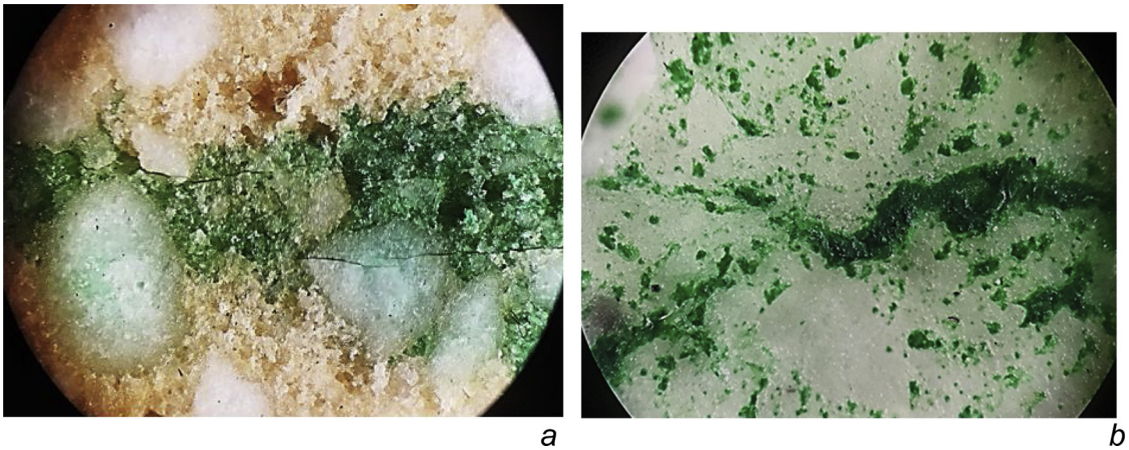

Fig. 8. Micrographs of cracks in the samples SB1-4 (a) and CFS1-1(b) after 50 thermal shocks.

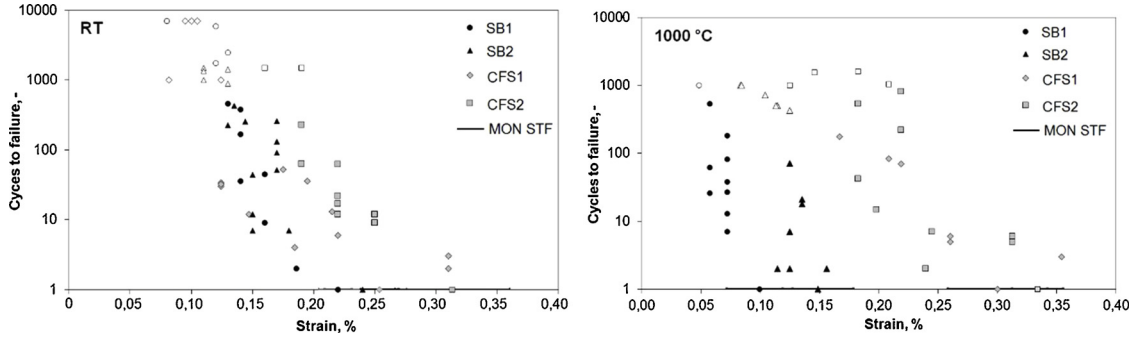

Fig. 9. Summary of fatigue results (a) RT (b) 1000 °C. MON STF shows the spread of monotonic strain at failure. Results when sample did not fail are shown as not filled signs.

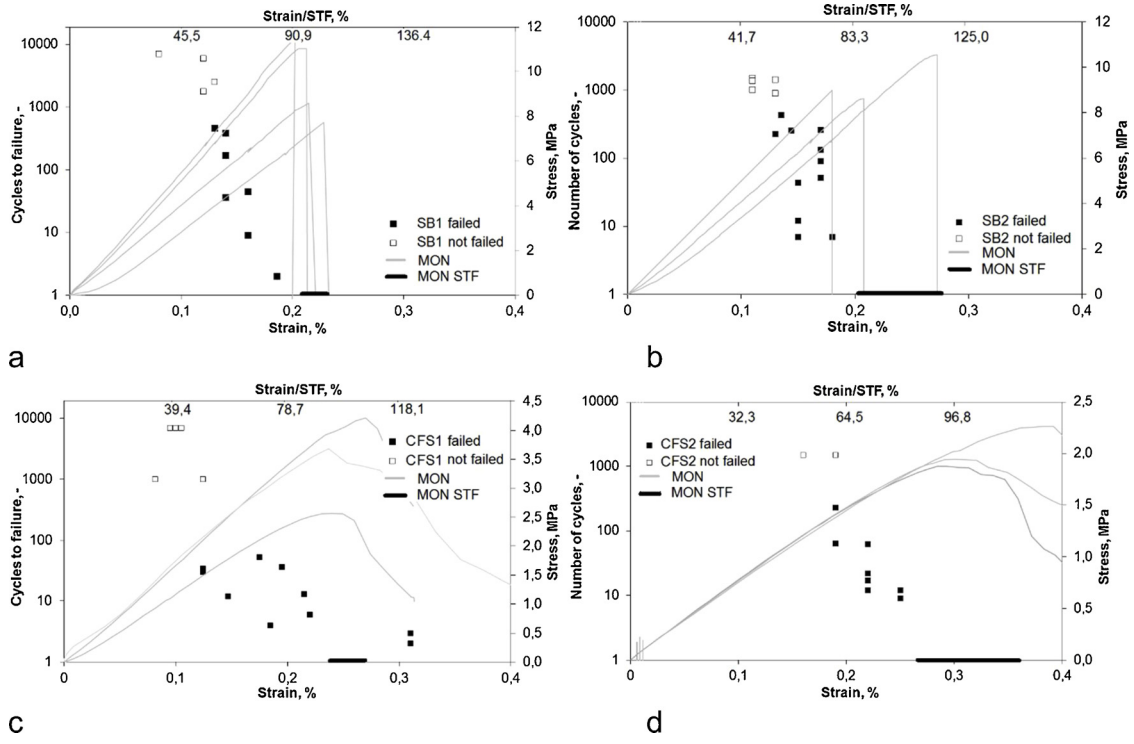

Fig. 10. Results of fatigue tests at RT (a) SB1 (b) SB2 (c) CFS1 (d) CFS2. MON STF - the spread of monotonic strain at failure. MON – monotonic stress-strain tests.

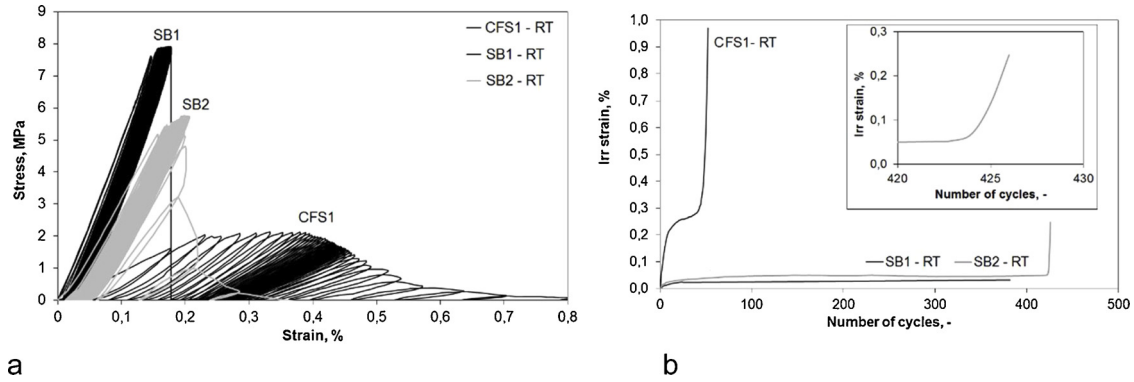

Fig. 11. Typical stress-strain curves of cyclic fatigue tests (a) and minimal strain per cycle vs cycle number (b). The amplitude is 70% of the strain at failure.

correlation of the strain at failure with the material brittleness (Fig. 5), the critical strains can be with some caution used as the indicators of the thermal shock resistance of the material.

There is a number of method specific issues relevant for correlating the service strain loads and the material properties. Monotonic loading measurements do not quantify the cycles to failure. For quasi-brittle materials (e.g. civil engineering masonry and concrete) to which refractory are microstructurally related it is known that the zone of fracture interaction is larger for cyclic (fatigue) than for monotonic loading [40]. These may influence the values of fracture energy

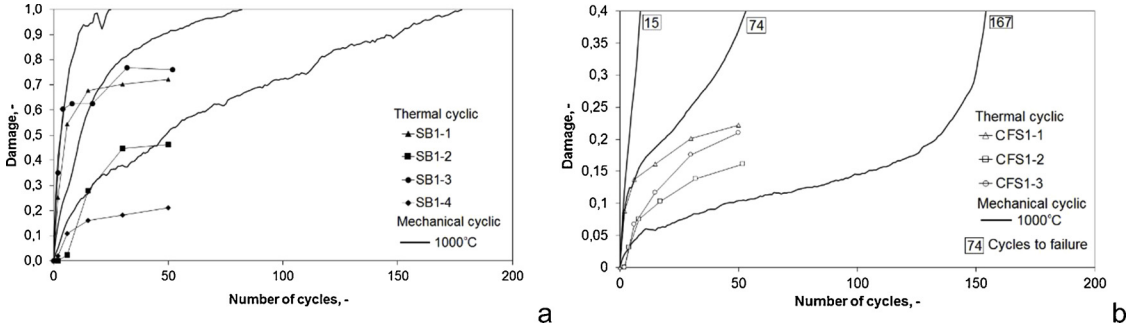

Fig. 12. Damage development due to thermal shock cycles and mechanical cyclic tests (a) SB1 (b) CFS1.

consumed in different loading modes. However the monotonic loading methods are most advanced in terms of methodology and interpretation of the results. There are indications that the limit strain values obtained from such methods can define the strain limits of the mechanical fatigue resistance trends [27,38].

The thermal shock test has an advantage that it accounts for all the material properties critical for thermal shock resistance. The test is quite similar to the in-service wear conditions. However, the predictions regarding the number of shocks to failure cannot be translated to the lining wear. Potential differences between the test and the practice in the dimensions, thermal and mechanical boundary conditions define the abstract nature of the test results. To enable the link to in-service loads one can try measuring strains developing during the test or to quantify them using computer model. Another interesting question is whether the saturation of the damage frequently reported for the thermal shock tests is permanent, or in certain cases it is the secondary phase of the degradation as it is seen in the mechanical fatigue tests.

Thermal conductivity and expansion in SB1 and CFS1 are quite similar. During the thermal shock tests roughly similar strains are expected to develop in the samples of two materials. Regarding the outcome of the thermal shock tests for SB1 the strain realised in the test should be close to the strain at failure. The same strain for CFS1 was rather low in comparison with respective strain at failure. The few cracks observed on the surface of CFS1 samples did not show major effect either on strength or Young's modulus. The thermal shock tests on SB1 and CFS1 should be compared with the mechanical cyclic tests when samples failed after low and high number of cycles, respectively (Fig. 12). For CFS1 the damage curves of the two methods have certain similarity. For SB1 the similarity is seen during the lower cycles. During higher cycles the rates of damage accumulation in the thermal test seems to be much lower. Comparing the damage of the two cyclic methods one should remember that for different methods different properties were used to quantify it. In addition in thermal tests the damage develops at changing temperature and therefore in the microstructure of the changing condition. In the mechanical tests the damage develops at one temperature.

The mechanical fatigue test has a potential to combine the benefits of the both above approaches. It allows direct correlation of loads and material response in the stress—strain coordinates. It can quantify the degradation due to repetitive cycles. However in strain controlled fatigue tests the potential for the damage saturation depends on the loading protocols [13]. In tests with fixed maximal strain the development of irreversible strains results in the reduction of the effective loading amplitude. Thus the potential for the damage saturation is rather high here. In tests with constant effective strain amplitude the maximal strain grows with the damage development. This approach was used in the present study. The apparent damage saturation occurs here only in no failure samples of low amplitude. The utilisation of the latter approach is built on the assumption that the loading strains stay constant in the process of thermal shock and that the friction between the faces of the formed (micro-)cracks prevents the closure of the crack that promotes build-up of the irreversible strains. Whether this assumption is applicable to the whole process of the crack formation and growth under the thermal shock conditions needs to be proven by the observations of the thermal shock tests.

4. Conclusions

In amorphous (as received) form the fused silica materials are rather brittle. Their high thermal shock resistance is guaranteed by the low coefficient of thermal expansion. Crystallised fused silica materials of the morphology realised in the used heat treatment regime have high strain tolerance and low brittleness that promotes resistance to the crack growth and thermal shock. These properties result from the tendency to form more tortuous crack path that avoids larger grains and are formed by the micro-cracks. Differences in performance between the materials within one type are seen to be lower than those between the types.

Utilised alternative methods produce same ranking for the studied materials. The mechanical strain controlled fatigue tests allow direct correlation of the loads and material response in the stress—strain coordinates. At the same time it allows monitoring the material degradation during the repetitive loading cycles. As a result it combines the benefits of the thermal shock tests and stress-strain tests of monotonic loading. The critical strain is the laboratory test parameter that can correlate the material behaviour observed in tests of different methods and the loads specific for the service. Further work is to concentrate on the correlation of thermal shock and mechanical cyclic (fatigue) tests for the wide range of the refractories and on the specifying potential cyclic degradation limits using established fracture mechanics tests.

Conflict of interest

The authors declare no conflict of interest.

Acknowledgements

Financial support from the open fund (G201701) of The State Key Laboratory of Refractories and Metallurgy, Wuhan University of Science and Technology (WUST) "Thermo-mechanical behaviour of alternative refractories for coke oven walls", ETH-ATHOR project (No 764987) is gratefully acknowledged by the co-authors from WUST and RWTH University, respectively.

References

[1] W.D. Kingery, Factors affecting thermal stress resistance of ceramic materials, J. Am. Ceram. Soc. 38 (1) (1955) 3–15.
[2] D.P.H. Hasselman, Thermal stress resistance parameters for brittle refractory ceramics: a compendium, Am. Ceram. Soc. Bull. 49 (12) (1970) 1033–1037.
[3] H. Harmuth, R.C. Bradt, Investigation of refractory brittleness by fracture mechanical and fractographic methods, Interceram. Refract. Manual 1 (2010) 6–10.
[4] R.C. Bradt, C.A. Schacht (Ed.), Fracture of Refractories p11-38 in Refractories

Handbook, Marcel Dekker, New York, 2004.
[5] Standard CEN/TS 993-11, Dense Shaped Refractory Products – Part 11: Determination of Resistance to Thermal Shock; German Version. 2003, Beuth Verlag GmbH, Berlin, 2003.
[6] Y. Hino, Y. Kiyota, Fatigue failure and thermal spalling tests to evaluate dynamic fatigue fracture of MgO–C bricks, ISIJ Int. 51 (11) (2011) 1809–1818 water quenching.
[7] T. Arahori, T. Suzuki, K. Fujisawa, Mechanical behavior of silica refractories under thermal cycle, Yogyo-Kyokai-Shi 91 (11) (1985) 32–39.
[8] J. Schnieder, N. Traon, S. Etzold, T. Tonnesen, R. Telle, A. Tengstrand, A. Malmgren, E. Nylund, Fracture process zone in refractory castables after high-temperature thermal shock, Refract. World Forum 8 (2016) 74–80.
[9] E.D. Case, The saturation of thermo-mechanical fatigue damage in brittle materials. 137-208, in: M.H. Aliabadi (Ed.), Thermo-Mechanical Fatigue and Fracture, WIT-Press, Southampton, Boston, 2002.
[10] Y. Hino, K. Yoshuda, Y. Kiyota, M. Kuwayama, Fracture mechanics investigation of MgO–C bricks for steelmaking by bending and fatigue failure fests along with X-Ray CT scan observation, ISIJ Int. 53 (8) (2013) 1392–1400.
[11] E. Ouedraogo, N. Prompt, High-temperature characterisation of an alumina refractory concrete for blast furnace main trough. Part II. Material behaviour, J. Eur. Ceram. Soc. 28 (2008) 2867–2875.
[12] F. Thummen, C. Olagnon, N. Godin, Cyclic fatigue and lifetime of a concrete refractory, J. Eur. Ceram. Soc. 26 (2006) 3357–3363.
[13] K. Andreev, V. Tadaion, J. Koster, E. Verstrynge, Cyclic fatigue of silica refractories - effect of test method on failure process, J. Eur. Ceram. Soc. 37 (4) (2017) 1811–1819.
[14] K. Andreev, M. Boursin, A. Laurent, E. Zinngrebe, P. Put, S. Sinnema, Compressive fatigue behaviour of refractories with carbonaceous binders, J. Eur. Ceram. Soc. 34 (2) (2014) 523–531.
[15] Ju.K. Malishkin, I.P. Basjas, Fatigue of magnesia based refractories at high temperatures, Refractories 8 (1972) 51–54 (In Russian).
[16] Y. Hino, Y. Kiyota, Fatigue failure behaviour of Al2O3–SiO2 system bricks under compressive stress at room and high temperatures, ISIJ Int. 52 (6) (2012) 1045–1053.
[17] S.S. Manson, Thermal Stress and Low Cycle Fatigue, McGraw-Hill Book Company, New York, 1966.
[18] A. Fissolo, C. Robertson, V. Maillot, Prediction of crack initiation and growth in thermal fatigue 68-105, in: M.H. Aliabadi (Ed.), Thermo-Mechanical Fatigue and Fracture, WIT-Press, Southampton, Boston, 2002.
[19] Y. Shinohara, Refractories Handbook, Japanese Association of Refractories, Tokyo, 1998.
[20] A. Yamaguchi, Fundamentals and micro-structure of silica bricks, J. Tech. Assoc. Refract. Japan 31 (3) (2011) 148–151.
[21] K. Andreev, M.V. Wijngaarden, P. Put, V. Tadaion, O. Oerlemans, Refractories for Coke Oven Wall – Operator's Perspective, Berg- und Huettenmaennische Monatshefte, 2016, https://doi.org/10.1007/s00501-016-0563-6.
[22] S. Hosohara, Damage of Coke Oven Refractories. Shinagava Technical Report 59 (2016), pp. 20–30.
[23] E. Gregorova, M. Cerny, W. Pabst, L. Esposito, C. Zanelli, J. Hamacek, J. Kutzendoerfer, Temperature dependence of Young's modulus of silica refractories, Ceram. Int. 41 (2015) 1129–1138.
[24] W. Pabst, E. Gregorova, Elastic properties of silica polymorths – a review, Ceramics-Silikaty 57 (3) (2013) 167–184.
[25] P. Pilate, V. Lardot, F. Cambier, E. Brochen, Contribution to the understanding of the high temperature behaviour and of the compressive creep behaviour of silica refractory materials, J. Eur. Ceram. Soc. 35 (2015) 813–822.
[26] N. Higashikawa, S. Nishida, M. Iida, Wide variety in monolithic refractories and precast block for coke oven, Shinagawa Tech. Rep. 59 (2016) 59–70.
[27] K. Andreev, N. Shetty, E. Verstrynge, Acoustic emission based damage limits and their correlation with fatigue resistance of refractory masonry, Constr. Build. Mater. 165 (2018) 639–646.
[28] E.K. Tschegg, Testing device and appropriate specimen shapes for tests to measure fracture values (in German), Austrian Patent Specification AT 390 328, J. Eur. Ceram. Soc. 38 (2018) 5601–5609.
[29] H. Harmuth, K. Rieder, M. Krobath, E. Tschegg, Investigation of non-linear fracture behaviour of ordinary ceramic refractory materials, Mater. Sci. Eng. A-Struct. 214 (1) (1996) 53–61.
[30] A. Majdic, L. Hagemann, G. Maercker, E. Overkott, A. Suckow, Thermal expansion of silica bricks for coke oven construction, Keram. Z. 34 (1982) 89–92.
[31] A. Sibil, J.P. Erauw, F. Cambier, M. R'Mili, N. Godin, G. Fantozzi, Study of damage of high zirconia fused-cast refractories by measurement of Young's modulus, Mater. Sci. Eng. A 521–522 (2009) 221–223.
[32] T. Zhu, Y. Li, Sh. Sang, Zh. Xie, Fracture behaviour of low carbon MgO–C refractories using the wedge splitting test, J. Eur. Ceram. Soc. 37 (4) (2017) 1789–1797.
[33] S. Ushida, K. Ikegami, Features of silica bricks used in coke ovens for 44 years, Shinagawa Tech. Rep. 59 (2016) 39–49.
[34] G. Briche, N. Tessier-Doyen, M. Huger, T. Chotard, Investigation of the damage behaviour of refractory model materials at high temperature by combined pulse echography and acoustic emission techniques, J. Eur. Ceram. Soc. 28 (2008) 2835–2843.
[35] T.J. Lu, N.A. Fleck, The thermal shock resistance of solids, Acta Mater. 46 (13) (1998) 4755–4768.
[36] S. Martinovic, M. Vlahovic, T. Boljanac, J. Majstorovic, T. Vokov-Husovic, Influence of sintering temperature on thermal shock behaviour of low cement high alumina refractory concrete, Compos. Part B Eng. 60 (2014) 400–412.
[37] S. Martinovic, M. Dojcinovic, M. Dimitrijevic, A. Devecerski, B. Matovic, T. Volkov Husovic, Implementation of image analysis on thermal shock and cavitation resistance testing of refractory concrete, J. of Eur. Cer. Soc. 30 (2010) 3303–3309.
[38] K. Andreev, N. Shetty, E. Verstrynge. Correlation of damage after first cycle with overall fatigue resistance of refractory castable concrete. Under review at J. Const. Build. Mat.
[39] Y. Dai, Y. Yin, X. Xu, S. Jin, Y. Li, H. Harmuth, Effect of the phase transformation on fracture behaviour of fused silica refractories, J. Eur. Ceram. Soc. 38 (2018) 5601–5609.
[40] R.O. Ritchie, Mechanisms of fatigue-crack propagation in ductile and brittle solids, Int. J. Fract. 100 (1999) 55–83.